Journal of BUON **17:** 57-64, 2012

ORIGINAL ARTICLE

Dynamic MRI-derived parameters for hot and cold spots: correlation with breast cancer histopathology

Dongfeng He, Daqing Ma, Erhu Jin

Department of Radiology, the Affiliated Beijing Friendship Hospital of Capital Medical University, Beijing, P.R. China

Summary

Purpose: *To identify the dynamic contrast-enhanced magnetic resonance (DCE-MR) imaging features that may predict the outcome of patients with breast cancer.*

Methods: *DCE-MR images from 87 patients newly diagnosed with primary breast cancer were reviewed. The kinetic parameters (including cold spot, hot spot, and heterogeneity parameters) were derived from the DCE-MRI data. These parameters were used to thoroughly reflect the tumor status. The association of dynamic MR features (including kinetic and morphological features) with established prognostic indicators was evaluated.*

Results: *Malignant tumors with poor histomorphological indicators showed higher values of hot spot parameters (maximal initial Slope [$maxSlope_i$] and maximal Washout [maxWashout]), higher values of a heterogeneity parameter-initial slope ratio ($Slope_i$ ratio) and lower values of a cold spot parameter (minimal initial slope [$minSlope_i$]) than those with favorable prognostic indicators. The heterogeneous internal enhancement pattern and rim-like enhancement pattern were more frequently observed in patients with poor prognostic indicators. Moreover, binary logistic regression analysis showed that kinetic parameters $Slope_i$ ratio ($p=0.021$), $minSlope_i$ ($p=0.024$), internal homogeneity ($p=0.001$), and $maxSlope_i$ ($p<0.001$) were independently and significantly associated with histological grade, lymph node status, tumor size, and Ki-67, respectively.*

Conclusion: *Our results suggest that all hot spot, cold spot, and heterogeneity parameters may be useful to noninvasively identify highly aggressive breast carcinomas. More importantly, cold spot and heterogeneity parameters may serve as crucial indicators to predict the outcome of breast cancer.*

Key words: breast cancer, dynamic MRI, MRI, prognosis

Introduction

To date, neoadjuvant chemotherapy for breast cancer has been more and more accepted [1,2]. It is important to predict the outcome of breast cancer for these patients prior to preoperative chemotherapy. Examination of the surgical specimens is one of the most important methods of predicting prognosis. However, for patients having undergone neoadjuvant chemotherapy this predictive method is impossible. Although core biopsy is always performed prior to chemotherapy, core biopsy specimens might not thoroughly reflect the status of the tumor due to local sampling. Therefore, we considered that a noninvasive approach was needed to assist clinicians in predicting breast cancer prognosis.

DCE-MRI, as a noninvasive approach, has been used to investigate the structure and function of tumor blood vessels. Some authors found that this imaging technique might have the potential of identifying highly aggressive breast cancer [3,4]. However, to the best of our knowledge, most of these studies focused on the evaluation of characteristics of hot spot. It is questionable whether the characteristics of hot spot fully describe the tumor.

It is believed that the breast tumor has not only the hot spot characteristics but also the cold spot and heterogeneity characteristics. The cold spot, which is difficult to attract the interest of radiologists, is always located in the depth of the tumor. The characteristics of cold spot indicate the features of an area with ischemia. One problem encountered in radiotherapy and chemotherapy is the lack of a sufficient oxygen and blood supply in

Correspondence to: Daqing Ma, MD. Department of Radiology, The Affiliated Beijing Friendship Hospital of Capital Medical University, No. 95 YongAn Road, Xuanwu District, Beijing 100050, P.R. China. Tel: +86 10 63138457/63138569, Fax: +86 10 63138457/63138569, E-mail: iceriverdr@sina.com.cn

Received 15-08-2011; Accepted 14-09-2011

these regions. On the other hand, the hot spot is always located in the periphery of tumor. The characteristics of hot spot indicate the features of the area with a sufficient blood supply. In malignant tumors, a sufficient blood supply always indicates vigorous tumor cell proliferation. Stomper et al. [5] found an association between peripheral enhancement and a high S-phase percentage of tumor cells which was an indicator of tumor proliferation. Moreover, some studies revealed the association of hot spot characteristics with prognostic indicators for breast cancer [4,6]. Breast cancer is also characterized by uneven distribution of vessels within the lesion, which is referred to here as tumor heterogeneity. Some studies [4,7] found that the internal heterogeneous enhancement pattern was more frequently observed in malignant tumors with poor prognostic indicators. Therefore, to thoroughly reflect the status of the tumor, not only the hot spot characteristics but also the cold spot and heterogeneity characteristics might also be evaluated.

The purpose of the present study was to identify DCE-MR imaging features that may predict the outcome of breast cancer. In this analysis, we correlated architectural parameters (including internal homogeneity and rim enhancement) and kinetic parameters (including cold spot, hot spot, and heterogeneity parameters) with established prognostic indicators.

Methods

Patients

Analysed were 87 patients (median age 57.0 years, range 35-82) newly diagnosed with primary malignant breast tumors by core biopsy from January 2008 through June 2008. Written informed consent was obtained from all patients prior to MRI examinations, and the institutional ethics committee approved our protocol. Table 1 shows the tumors' histopathological features.

MR imaging

The MR images were acquired on a 3.0T scanner (Signa Excite HD, GE Medical Systems, Milwaukee, Wisconsin) using a dedicated double breast coil. Patients were scanned in prone position. Transverse T1-weighted (T1W) fast spin-echo images and axial and sagittal T2-weighted (T2W) short-time inversion-recovery (STIR) images were obtained. Next, a dynamic examination with one pre-contrast and 12 post-contrast series was performed at 42-sec intervals, using a 3D liver accelerated volume acquisition (3DLAVA) sequence in the axial plane (TR 5.6 ms, TE 2.6 ms, TI 5.0 ms, flip angle 15°, field of view 34×34 cm, matrix 448×352, BW 62.5 kHz, ZIP×2, section thickness 3.2 mm). Images were reconstructed with 50% overlap. Before the post-contrast scans were collected, a bolus injection of gadolinium-diethylenetriaminepentaacetic acid (0.1 mmol/kg) was administered using a power injector within 15 sec. The total scan time was 9 min and 26 sec.

MR image analysis

Retrospective analysis of the morphological and kinetic data was jointly performed by 2 experienced radiologists who were blind to disease information. In 11 patients with multicentric carcinoma, the study was confined to the largest malignant lesion [8]. Signal intensities were obtained at precontrast and each postcontrast series using operator-defined regions of interest (ROIs). Measurements were performed in at least 3 areas with high contrast uptake, and in at least 3 areas with low contrast uptake. Of these measurements, the maximally and minimally enhancing ROIs (hot and cold spot) were selected for analysis [7,8]. The ROIs should be small enough (4-10 pixels) to exclude partial volume effects.

Table 2 shows the calculation methods of the parameters $Slope_i$ and Washout [7-9]. The cold spot, hot spot and heterogeneity parameters were calculated as follows:

1. $minSlope_i$= $Slope_i$ value of cold spot; minWashout=Washout value of cold spot.
2. $maxSlope_i$= $Slope_i$ value of hot spot; maxWashout= Washout value of hot spot
3. $Slope_i$ ratio= $maxSlope_i$/ $minSlope_i$; Washout ratio= (maxWashout- minWashout)/ maxWashout

To avoid bias, the calculations of all parameters were completed and documented before the biopsy, surgery, and histology procedures.

Analysis of MR morphology

Morphological features (including lesion distribution, inter-

Table 1. Histopathological features

Tumor histology	*No. of patients (%)*	*Mean diameter (cm) (range)*
Ductal carcinoma *in situ*	4/87 (4.6)	1.26 (0.83-2)
Invasive ductal carcinoma	78/87 (89.7)	2.53 (1.15-6.7)
Mucinous carcinoma	4/87 (4.6)	3.05 (2.0-4.1)
Malignant mesenchymoma	1/87 (1.1)	1.5

Table 2. Calculation methods of MR enhancement parameters [7-9]

Parameter	*Calculation*	*Definition*
En	En = (SIn-Sibase)/SIbase	Relative improvement in SI at each postcontrast measurement compared with the precontrast phase
$Slope_i$	$Slope_i$ = Enpeak/Tpeak	Rate of change of contrast enhancement from the precontrast phase up to the peak
Washout	Washout = (SIpeak -SI12)/SI12	Relative decrease in maximal SI compared with the last postcontrast phase

En: enhancement ratio, n=1-12; SI: signal intensity, SIbase: precontrast signal intensity, $Slope_i$: initial slope, T_{PEAK}: time elapsed between the administration of contrast agent and the phase at which the maximal SI value was obtained

nal homogeneity and rim-like enhancement) were evaluated based on models described by Nunes et al. [10] and Schnall et al. [11]. Tumor size was determined by measuring the longest diameter of the tumor on DCE-MR imaging.

Histopathological and immunohistological analysis

The representative samples of the tissue were routinely processed and stained with a standard hematoxylin-eosin method. Tumor grade was defined in all invasive adenocarcinomas according to the Scarf-Bloom-Richardson protocol as modified by Elston and Ellis [12,13] To avoid any influence from chemotherapy and local sampling, 38 patients without preoperative chemotherapy were selected from 82 patients with invasive adenocarcinomas to analyse their histological grading results based on surgical specimens. Lymph nodes (LNs) with detected metastasis of any size were considered as positivity. Histopathological features were analysed by two experienced pathologists. Core biopsy specimens were used for immunohistological examination.

The cut-off value for estrogen receptor (ER) positivity was 10% and for Ki-67 positivity 20%. The c-erbB-2 protein expression was semi-quantitatively assessed according to the study by Szabo et al. [7].

Statistical analysis

Because of skewed distributions, we used median and quartiles for the description of continuous data. To present categorical data, absolute and relative frequencies were given. To test whether two groups were drawn from the same population, the Mann-Whitney U test was performed; and for more than two groups, the Jonckheere Terpstra test was used. The Chi-square test was performed for all categorical data. Spearman correlation coefficients (r values) were calculated to quantify the correlation between two continuous variables. In order to find the most significant and independent relationships, binary logistic regression analysis with stepwise forward-likelihood-ratio variable selection was performed. The enter limit and remove limit for the regression models were 0.05 and 0.1, respectively. Statistical software (SPSS, version 12.0; SPSS Chicago, IL, USA) was used for the analyses above. For all tests, a p-value of <0.05 was considered statistically significant.

Results

Histopathological analysis

Of 38 patients with histological grading results, 9 (23.7%) had histological grade I tumor, 19 (50.0%) grade II, and 10 (26.3%) grade III. Of 87 patients with malignant breast tumor, 43 (49.4%) had LN metastasis and 43 (49.4%) had large tumor size (>2 cm). Among 85 patients with immunohistological results, there were 61 (71.8%) patients with ER (+), 42 (49.4%) with Ki-67 (+), and 35 (41.2%) with c-erbB-2 (+) status.

Analysis of MR morphology

All breast lesions were described as focal masses on the MR images. Of the 87 studied lesions, there were 24 (27.6%) lesions with rim-like enhancement. Homogeneous internal enhancement pattern was found in 11 (12.6%) cases, intermediate in 37 (42.5%), and 39 (44.8%) showed inhomogeneous structure.

Association of kinetic parameters with prognostic indicators

As shown in Table 3, malignant tumors with histomorphological indications of poor prognosis showed higher values of hot spot parameters ($maxSlope_i$ and maxWashout), and lower values of a cold spot parameter ($minSlope_i$) than those with favorable prognostic indicators. However, no difference was seen in both minWashout and Washout ratio between malignant tumors with unfavorable and favorable prognostic indicators. There was no difference in all the MR enhancement parameters between c-erbB-2 (-) group and c-erbB-2 (+) group.

As shown in Table 4 and Figure 1, several MR enhancement parameters such as $minSlope_i$, $Slope_i$ ratio, minWashout and Washout ratio showed considerable correlation ($p<0.001$, $p<0.001$, $p=0.004$, and $p=0.002$, respectively), while the heterogeneity parameter $Slope_i$ ratio showed a moderate correlation ($r=0.516$) with tumor size. The hot spot parameters ($maxSlope_i$ and maxWashout) and tumor size appeared not related to each other ($r=0.123$ and $r=0.130$, respectively).

Association of morphological features with prognostic indicators

The presence of rim-like enhancement was more often seen in the malignant tumors with a larger tumor size (Table 5, $p=0.014$). The presence of heterogeneous enhancement was more frequently observed in malignant tumors with poor prognostic indicators such as a higher histological grade ($p=0.030$), larger tumor size ($p<0.001$), and positive LN status ($p=0.016$).

Kinetic and morphological MR features to predict established prognostic indicators

Variables found to be significant at the univariate analysis (Mann-Whitney U test, Jonckheere Terpstra test, Chi-square test, or Spearman correlation test), were selected for logistic regression analysis. Four regression models were created using histological grade, LN status, tumor size and Ki-67 expression as the dependent variable, respectively. $MinSlope_i$, $Slope_i$ ratio, and internal homogeneity were used for the regression model for histological grade and LN status. Cold spot

Table 3. Difference in kinetic parameters between malignant lesions with favorable and unfavorable prognostic indicators

Indicator and p-value	*Cold spot parameters*		*Hot spot parameters*		*Heterogeneity parameters*	
Histological grade	$MinSlope_i$	MinWashout	$MaxSlope_i$	MaxWashout	$Slope_i$ ratio	Washout ratio
1	0.0061 (0.0039,0.0075)	0.0268 (0.0046,0.0966)	0.0488 (0.0312,0.0696)	0.3759 (0.2584,0.4810)	6.6250 (5.1857,18.6917)	0.9016 (0.8101,0.9883)
2	0.0054 (0.0026,0.0084)	0.0139 (0.0000,0.0277)	0.0388 (0.0254,0.0553)	0.3303 (0.2461,0.3985)	9.7692 (5.3063,10.6452)	0.9405 (0.9118,1.0000)
3	0.0014 (0.0010,0.0055)	0.0031 (0.0000,0.0336)	0.0529 (0.0400,0.0748)	0.3433 (0.2373,0.3887)	17.6238 (10.1774,53.8352)	0.9908 (0.9117,1.0000)
p-value	0.025	0.109	0.611	0.466	0.031	0.122
Lymph node status						
Negative	0.0061 (0.0038,0.0086)	0.0252 (0.0000,0.0538)	0.0461 (0.0280,0.0588)	0.2939 (0.2442,0.3906)	6.5890 (4.4627,11.3711)	0.9231 (0.8291,1.0000)
Positive	0.0040 (0.0026,0.0060)	0.0000 (0.0000,0.0657)	0.0434 (0.0295,0.0683)	0.3578 (0.2728,0.4203)	10.7750 (7.9811,14.8571)	1.0000 (0.8313,1.0000)
p-value	0.013	0.138	0.812	0.109	0.009	0.058
Estrogen receptor status						
Negative	0.0055 (0.0036,0.0106)	0.0239 (0.0015,0.0677)	0.0536 (0.0320,0.0740)	0.3433 (0.2692,0.4186)	7.7781 (4.0493,13.2079)	0.9224 (0.8290,0.9954)
Positive	0.0051 (0.0024,0.0066)	0.0072 (0.0000,0.0526)	0.0423 (0.0291,0.0537)	0.3071 (0.2454,0.4059)	9.7778 (5.6636,13.5337)	0.9816 (0.8297,1.0000)
p-value	0.088	0.145	0.106	0.696	0.237	0.162
Ki-67						
Negative	0.0044 (0.0022,0.0068)	0.0053 (0.0000,0.0538)	0.0333 (0.0216,0.0485)	0.2827 (0.2153,0.3710)	9.4355 (4.8382,12.8750)	0.9816 (0.8230,1.0000)
Positive	0.0055 (0.0032,0.0087)	0.0237 (0.0000,0.0605)	0.0537 (0.0425,0.0748)	0.3771 (0.2808,0.4652)	9.6746 (5.4932,14.2284)	0.9375 (0.8305,1.0000)
p-value	0.179	0.247	<0.001	0.001	0.623	0.518
c-erbB-2						
Negative	0.0051 (0.0026,0.0074)	0.0027 (0.0000,0.0520)	0.0430 (0.0298,0.0592)	0.3444 (0.2456,0.4182)	10.0889 (5.6469,13.0396)	0.9908 (0.8297,1.0000)
Positive	0.0054 (0.0028,0.0084)	0.0159 (0.0000,0.0638)	0.0485 (0.0295,0.0655)	0.3036 (0.2676,0.3868)	8.0833 (4.4754.14.8571)	0.9405 (0.8281,1.0000)
p-value	0.744	0.255	0.639	0.550	0.526	0.255

Except for p-values, data are median; data in parentheses are 25th and 75th percentiles

parameters ($minSlope_i$ and minWashout), heterogeneity parameters ($Slope_i$ ratio and Washout ratio), and morphological features (rim enhancement and internal homogeneity) were analysed in the tumor size model.

Table 4. Spearman's correlation coefficient (r) between kinetic parameters and tumor size

MR parameters	*Correlation coefficient (r)*	*p-value*
$MinSlope_i$	–0.442	<0.001
$MaxSlope_i$	0.123	0.258
$Slope_i$ ratio	0.516	<0.001
MinWashout	–0.302	0.004
MaxWashout	0.130	0.231
Washout ratio	0.331	0.002

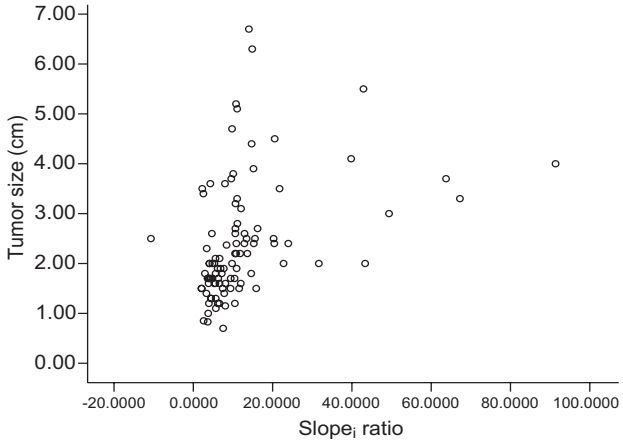

Figure 1. $Slope_i$ ratio correlated significantly with tumor size (p<0.001).

Table 5. Association between the morphological characteristics and prognostic indicators for malignant lesions

Indicator and p-value	*Rim enhancement*		*Internal homogeneity*		
Histological grade	Present	Absent	Homogeneous	Intermediate	Heterogeneity
1	1/9 (11.1)	8/9 (88.9)	2/9 (22.2)	5/9 (55.6)	2/9 (22.2)
2	5/19 (26.3)	14/19 (73.7)	1/19 (5.3)	12/19 (63.2)	6/19 (31.6)
3	6/10 (60.0)	4/10 (40.0)	0/10 (0.0)	2/10 (20.0)	8/10 (80.0)
p-value	0.071		0.030		
Tumor size (cm)					
≤2	7/44 (15.9)	37/44 (84.1)	11/44 (25.0)	23/44 (52.3)	10/44 (22.7)
>2	17/43 (39.5)	26/43 (60.5)	0/43 (0.0)	14/43 (32.6)	29/43 (67.4)
p-value	0.014		<0.001		
Lymph node status					
Negative	10/44 (22.7)	34/44 (77.3)	9/44 (20.5)	21/44 (47.7)	14/44 (31.8)
Positive	14/43 (32.6)	29/43 (67.4)	2/43 (4.7)	16/43 (37.2)	25/43 (58.1)
p-value	0.305		0.016		
Estrogen receptor status					
Negative	7/24 (29.2)	17/24 (70.8)	2/24 (8.3)	14/24 (58.3)	8/24 (33.3)
Positive	16/61 (26.2)	45/61 (73.8)	9/61 (14.8)	23/61 (37.7)	29/61 (47.5)
p-value	0.784		0.220		
Ki-67					
Negative	11/43 (25.6)	32/43 (74.4)	8/43 (18.6)	14/43 (32.6)	21/43 (48.8)
Positive	12/42 (28.6)	30/42 (71.4)	3/42 (7.1)	23/42 (54.8)	16/42 (38.1)
p-value	0.756		0.077		
c-erbB-2					
Negative	12/50 (24.0)	38/50 (76.0)	6/50 (12.0)	22/50 (44.0)	22/50 (44.0)
Positive	11/35 (31.4)	24/35 (68.6)	5/35 (14.3)	15/35 (42.9)	15/35 (42.9)
p-value	0.448		0.953		

Data in parentheses are percentages

The effect of hot spot parameters ($maxSlope_i$ and maxWashout) was evaluated in the Ki-67 model. Since no variables showed a significant correlation with ER and c-erbB-2 expression, we did not create regression models for these two indicators.

Table 6 shows the results of multiple logistic regression models. $Slope_i$ ratio was the only significant and independent predictor for histological grade (p=0.021), while $minSlope_i$ correlated with LN status (p=0.024). The only independent predictor for tumor size was internal homogeneity (p<0.001). $MaxSlope_i$ also retained its significance in predicting Ki-67 status (p=0.001). A 1 unit increase in $Slope_i$ ratio was associated with a 5.2% increase in the odds of high histological grade. A 1 grade increase in internal homogeneity was associated with 5.42-fold increase in the odds of large tumor size. A 0.001 unit increase in $minSlope_i$ was associated with a 12.6% decrease in the odds of LN involvement. A 0.001 unit increase in $maxSlope_i$ was associated with a 3.8% increase in the odds of being Ki-67 (+). Figure 2 shows an example of identifying highly aggressive breast cancer by evaluation of morphological features, hot spot characteristics, and cold spot characteristics. The malignant lesion with relatively high histological grade showed a slow enhancement pattern at the cold spot. However, the 3 malignant lesions seemed to have a similarly rapid enhancement pattern at hot spot and a similar rim-like enhancement pattern.

Discussion

To date, most DCE-MRI studies have focused on the analysis of DCE-MRI data from the region with the highest enhancement (which was referred to here as the hot spot) [3,14]. The time-signal intensity curve (TIC)

Table 6. Results of logistic regression analysis models of histological grade, tumor size, lymph node (LN) status, and Ki-67 status

Dependent variable	*First independent variable (β)*	*p-value*	*Second independent variable*
Histological grade (I+II vs. III)	$Slope_i$ ratio (0.051)	0.021	not applicable
Tumor size (≤2 vs. >2 cm)	Internal homogeneity (1.860)	<0.001	not applicable
LN status	$MinSlope_i$ (–134.372)	0.024	not applicable
Ki-67 status	$MaxSlope_i$ (37.624)	0.001	not applicable

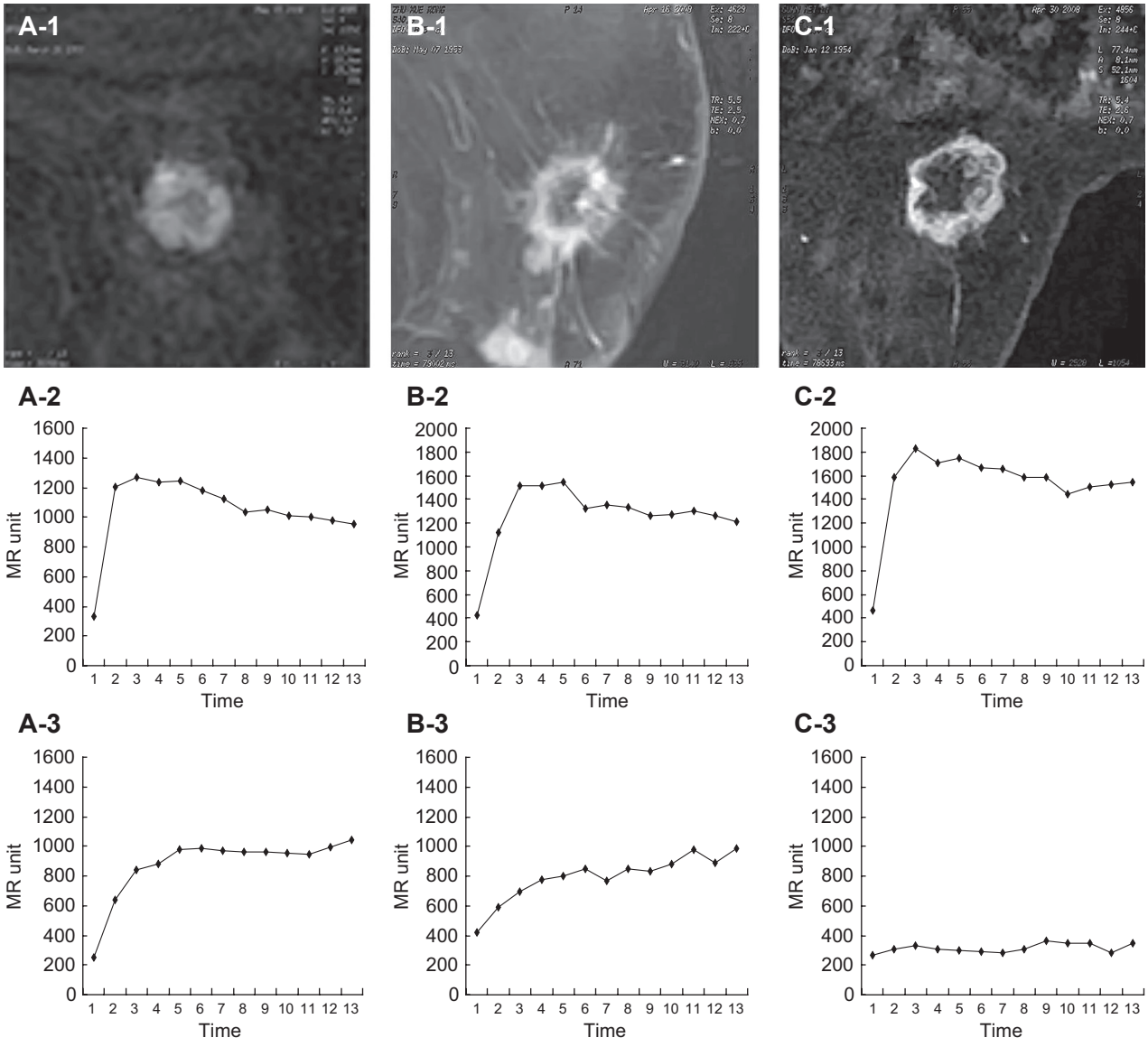

Figure 2. A (1-3), **B** (1-3), and **C** (1-3) were obtained from malignant tumors with histological grade I, II, and III, respectively. A-1, B-1, and C-1 show that all these tumors have an appearance of rim-like enhancement. A-2, B-2, and C-2 show that a rapid enhancement appears at the hot spot of all these tumors. These figures indicate that these malignant tumors seem to have similar characteristics of hot spot and similar morphological features. However, A-3, B-3, and C-3 show that a slower enhancement appears at the cold spot of the malignant tumor with a higher histological grade.

was generated from the hot spot. Then, the kinetic parameters were also derived from the TIC. Some authors [7,8] reported the potential prognostic value of these kinetic parameters. However, the characteristics of hot spot alone may not thoroughly reflect the status of the breast lesion.

It is believed that malignant breast tumors always contain the hot and cold spot. Based on the analytical results shown in this study, we hypothesised that not only the hot spot characteristics, but also the cold spot and heterogeneity characteristics should be evaluated to fully describe the status of breast tumor. Our findings may help clinicians to predict breast cancer prognosis and may provide useful information on formulating an individualized treatment plan. To the best of our knowledge, this study is the first DCE-MRI study evaluating the hot spot characteristics together with cold spot and heterogeneity characteristics for patients with breast cancer.

Prognostic factors of breast cancer

To date, besides LN status being the single most important prognostic factor, tumor size is also recognized as a powerful predictor for the outcome of the disease. Together with histological grade, these factors are categorized as classical pathological prognostic factors

[7,15-17]. The immunohistological prognostic factors include ER, Ki-67, and c-erbB-2. ER status in breast cancer is currently used to select patients for hormonal therapy and can also provide prognostic information [18]. Ki-67 is an excellent molecular marker of cell proliferation and proved to be a powerful and independent prognostic factor for patients with breast cancer [4]. C-erbB-2 is associated with poor prognosis and is routinely measured because of its value in predicting response to herceptin [19,20].

Prognostic values of cold spot, hot spot, and heterogeneity parameters

To date, few DCE-MRI studies have focused on the analysis of data from cold spot. However, some authors [21,22] have demonstrated that necrosis is a predictor of poor breast cancer prognosis. We consider that necrosis may be a special form of cold spot. In the present study, the cold spot parameters were used to evaluate the characteristics of the ischemic region of the malignant breast tumor. Our findings revealed that the cold spot of a malignant tumor with unfavorable prognostic indicators might be colder than that of a malignant tumor with favorable prognostic factors.

Blood vessels in tumor are distributed in an irregular pattern and do not follow the hierarchical branching pattern of normal vascular networks. Normal tissue maintains a balance between vascular growth and cellular demands—blood vessels will not be overgrown while at the meantime the distance from cells to the nearest blood vessel is always no farther than the distance the nutrients can diffuse before being completely consumed, so as to ensure the nutrition supply for all the cells. However, this balance is disrupted in tumors, which results in avascular and hypoxic voids of many sizes [23]. The ischemia-induced tumor necrosis may be considered as one of the important forms of cold spot. Jeong et al. [24] pointed out that hypoxia occurs frequently in various solid tumors and elicits a cellular response designed to improve cell survival through adaptive processes, thereby accelerating cancer progression and the development of chemotherapy resistance. Therefore, further study of evaluating such cold spot characteristics may contribute to an increase in the efficacy of chemotherapy or radiotherapy. On the other hand, we should note that the cold spot should be not only tumor necrosis but also "normal" ischemic area such as fibrosis. Evaluation of the status of different cold spots may play a different role in the prediction of breast cancer prognosis. Therefore, we should study the characteristics of cold spot further.

In the present study, hot spot parameters were used to evaluate the characteristics of the area with a sufficient blood supply. Our results showed that the hot spot parameter ($maxSlope_i$) correlated significantly with Ki-67 which was an indicator of cell proliferation. Bone et al. [25] and Mussurakis et al. [26] also found similar results to those of the present study.

The heterogeneity parameters were used to evaluate the characteristics of heterogeneity of the breast cancer. Angiogenesis constitutes a prerequisite for the growth of malignant tumors beyond a certain size. However, the microvessels are rarely distributed uniformly in malignant tumors. Teifke et al. [8] had placed one ROI in the peripheral area with the highest enhancement and another one was placed in the geometric center. They found: 1) a distinct increase of microvessel density from the center toward the periphery of malignant tumors; and 2) malignant tumors with histomorphological indications of a poor prognosis showed higher ratios of peripheral to central enhancement, higher washout rates, and earlier enhancement peaks than those with favorable prognostic indicators. These results were similar to ours. Our results showed that the heterogeneity parameter ($Slope_i$ ratio) was associated with histological grade. We also found that both the rim-like enhancement and the heterogeneous internal enhancement pattern were more frequently observed in the malignant tumors with poor prognostic indicators. These results were similar to some other reports [7,20]. It is likely that both the rim-like enhancement and the heterogeneous internal enhancement pattern might be the special forms of tumor heterogeneity.

Our study has some limitations. First, the sample size was small. Second, we did not evaluate the interobserver variability or the reproducibility of measurements of kinetic parameters. We selected at least 6 ROIs per lesion to reduce interobserver variability. Third, we did not evaluate the association between these kinetic parameters and the response to neoadjuvant chemotherapy. We should study it further.

In summary, the kinetic parameters (including hot spot, cold spot, and heterogeneity parameters) had the potential of identifying highly aggressive breast malignant tumor. To reflect the totality of malignant breast tumors, the cold spot should receive as much attention as the hot spot in the DCE-MRI analysis for patients with breast cancer.

Acknowledgement

This work was funded by the Capital Medical University. All authors acknowledge Mrs Zhang Yi and Mr Su Tianhao for their technical assistance.

References

1. Fisher ER, Wang J, Bryant J, Fisher B, Mamounas E, Wolmark N. Pathobiology of preoperative chemotherapy: findings from the National Surgical Adjuvant Breast and Bowel (NSABP) protocol B-18. Cancer 2002; 95: 681-695.
2. Rastogi P, Anderson SJ, Bear HD et al. Preoperative chemotherapy: updates of National Surgical Adjuvant Breast and Bowel Project Protocols B-18 and B-27. J Clin Oncol 2008; 26: 778-785.
3. Sinha S, Sinha U. Recent advances in breast MRI and MRS. NMR Biomed 2009; 22: 3-16.
4. Lee SH, Cho N, Kim SJ et al. Correlation between high resolution dynamic MR features and prognostic factors in breast cancer. Korean J Radiol 2008; 9: 10-18.
5. Stomper PC, Herman S, Klippenstein DL, Winston JS, Budnick RM, Stewart CC. Invasive breast carcinoma: analysis of dynamic magnetic resonance imaging enhancement features and cell proliferative activity determined by DNA S-phase percentage. Cancer 1996; 77: 1844-1849.
6. Heldahl MG, Bathen TF, Rydland J et al. Prognostic value of pretreatment dynamic contrast-enhanced MR imaging in breast cancer patients receiving neoadjuvant chemotherapy: overall survival predicted from combined time course and volume analysis. Acta Radiol 2010; 51: 604-612.
7. Szabó BK, Aspelin P, Kristoffersen Wiberg M, Tot T, Boné B. Invasive breast cancer: correlation of dynamic MR features with prognostic factors. Eur Radiol 2003; 13: 2425-2435.
8. Teifke A, Behr O, Schmidt M et al. Dynamic MR imaging of breast lesions: correlation with microvessel distribution pattern and histological characteristics of prognosis. Radiology 2006; 239: 351-360.
9. Takeda Y, Yoshikawa K. Contrast-enhanced dynamic MR imaging parameters and histological types of invasive ductal carcinoma of breast. Biomed Pharmacother 2005; 59: 115-121.
10. Nunes LW, Schnall MD, Orel SG et al. Breast MR imaging: interpretation model. Radiology 1997; 202: 833-841.
11. Schnall MD, Rosten S, Englander S, Orel SG, Nunes LW. A combined architectural and kinetic interpretation model for breast MR images. Acad Radiol 2001; 8: 591-597.
12. Elston CW, Ellis IO. Pathological prognostic factors in breast cancer. I. The value of histological grade in breast cancer: experience from a large study with long-term follow-up. Histopathology 1991; 19: 403-410.
13. Elston CW, Ellis IO, Pinder SE. Pathological prognostic factors in breast cancer. Crit Rev Oncol Hematol 1999; 31: 209-223.
14. Kuhl CK, Mielcareck P, Klaschik S et al. Dynamic breast MR imaging: are signal intensity time course data useful for differential diagnosis of enhancing lesions? Radiology 1999; 211: 101-110.
15. Caudle AS, Gonzalez-Angulo AM, Hunt KK et al. Predictors of tumor progression during neoadjuvant chemotherapy in breast cancer. J Clin Oncol 2010; 28: 1821-1828.
16. Rozenowicz Rde L, Santos RE, Silva MA et al. Cox-2 and its association with prognostic factors and response to primary chemotherapy in patients with breast cancer. Rev Col Bras Cir 2010; 37: 323-327.
17. Razek AA, Gaballa G, Denewer A, Nada N. Invasive ductal carcinoma: correlation of apparent diffusion coefficient value with pathological prognostic factors. NMR Biomed 2010; 23: 619-623.
18. Bacci G, Picci P, Mercuri M et al. Premenopausal hormone-responsive breast cancer with extensive axillary nodes involvement: total estrogen blockade and chemotherapy. Anticancer Res 2011; 31: 671-676.
19. Callahan R, Hurvitz S. Human epidermal growth factor receptor-2-positive breast cancer: Current management of early, advanced, and recurrent disease. Curr Opin Obstet Gynecol 2011; 23: 37-43.
20. Jeh SK, Kim SH, Kim HS et al. Correlation of the apparent diffusion coefficient value and dynamic magnetic resonance imaging findings with prognostic factors in invasive ductal carcinoma. J Magn Reson Imaging 2011; 33: 102-109.
21. Yu L, Yang W, Cai X, Shi D, Fan Y, Lu H. Centrally necrotizing carcinoma of the breast: clinicopathological analysis of 33 cases indicating its basal-like phenotype and poor prognosis. Histopathology 2010; 57: 193-201.
22. Shek LL, Godolphin W. Model for breast cancer survival: relative prognostic roles of axillary nodal status, TNM stage, estrogen receptor concentration, and tumor necrosis. Cancer Res 1988; 48: 5565-5569.
23. Jain RK. Molecular regulation of vessel maturation. Nat Med 2003; 9: 685-693.
24. Jeong JK, Moon MH, Seo JS, Seol JW, Lee YJ, Park SY. Sulforaphane blocks hypoxia-mediated resistance to TRAIL-induced tumor cell death. Mol Med Report 2011; 4: 325-30.
25. Boné B, Aspelin P, Bronge L, Veress B. Contrast-enhanced MR imaging as a prognostic indicator of breast cancer. Acta Radiol 1998; 39: 279-284.
26. Mussurakis S, Buckley DL, Horsman A. Dynamic MR imaging of invasive breast cancer: correlation with tumour grade and other histological factors. Br J Radiol 1997; 70: 446-451.